

GEANT Simulation of the AGILE Gamma-Ray Imaging Detector

Veronica Cocco*, Francesco Longo[†] and Marco Tavani**

**Dip. di Fisica, Univ. di Roma "Tor Vergata" and INFN, sezione di Roma II, Italy*

[†]Dip. di Fisica, Univ. di Ferrara and INFN, sezione di Ferrara, Italy

***Istituto Fisica Cosmica, CNR, Milano, Italy*

Abstract. We present results obtained with a GEANT-based Simulator of the Gamma-Ray Imaging Detector (GRID) developed for the AGILE space astrophysics mission. We describe the AGILE instrument geometry and the model assumed for the charged particle and the albedo-photon backgrounds. Using this simulator, we optimized the event trigger processing. In this paper, we present the main results on different levels of data processing and obtain the background rejection efficiency and the GRID effective area for photon detection in the energy range ~ 30 MeV - 50 GeV.

INTRODUCTION

AGILE is an ASI Small Scientific Mission dedicated to high energy astrophysics [1]. The AGILE instrument is designed to detect and image photons in the 30 MeV - 50 GeV and 10 - 40 keV energy bands, with excellent spatial resolution and timing capability and an unprecedentedly large field of view covering $\sim 1/5$ of the entire sky at energies above 30 MeV. Primary scientific goals include the study of AGNs, gamma-ray bursts, Galactic sources, unidentified gamma-ray sources, diffuse Galactic gamma-ray emission, and high precision timing studies. The AGILE gamma-ray mission requires a low-background orbit to maximize its scientific output.

The optimization of the AGILE design was obtained through a Montecarlo study of the detector performance. Simulations were done using the GEANT 3.21 code [2] which traces all possible interactions of particles with the apparatus, and reliably takes into account the deposited energy in the instrument detectors.

In this paper, we describe the AGILE instrument and the particle/albedo-photon background models assumed for the optimization of the on-board data processing. We outline the adopted trigger strategies and present the main results about the on-board background rejection and photon-detection efficiency (a first step to obtain the effective area).

THE AGILE INSTRUMENT MODEL

The AGILE scientific instrument is made of three integrated detectors with broad-band detection and imaging capabilities [1, 3]. The AGILE Gamma-Ray Imaging Detector (GRID) consists of a Silicon-Tungsten Tracker, a Cesium Iodide Mini-Calorimeter, an

Anticoincidence system made of segmented plastic scintillators, fast readout electronics and processing units. The Super-AGILE detector will provide detection and imaging capabilities in the hard X-ray range. It consists of an additional plane of four Silicon square units positioned on the top of the GRID Tracker plus an ultra-light coded mask structure with a top absorbing mask at a distance of 14 cm from the Silicon detectors. The CsI Mini-Calorimeter will also detect and collect events independently from the GRID in case of impulsive transients.

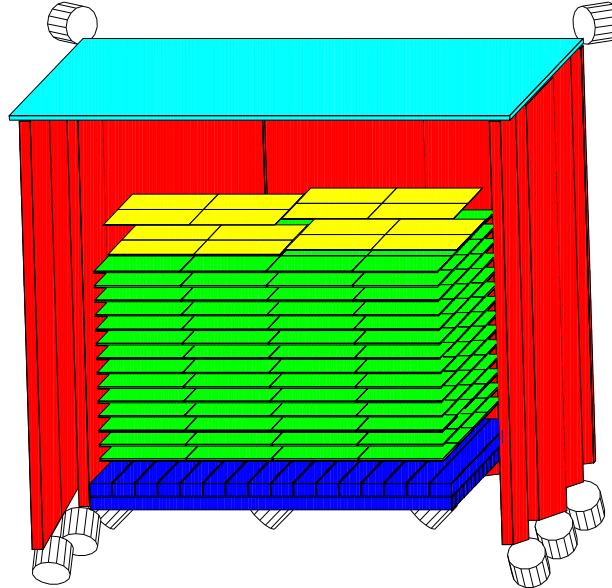


FIGURE 1. A simplified view of the AGILE instrument model. The Super-AGILE coded mask structure, the mechanical structure and the lateral electronics boards are not shown.

GRID. In the simulation code we modelled the GRID detector according to the AGILE design [3]. The Silicon Tracker is made of 14 detection planes with a distance between consecutive planes of 1.6 cm. Each plane is composed of two layers of 16 silicon tiles with a surface of $9.5 \times 9.5 \text{ cm}^2$ each and with a thickness of $410 \mu\text{m}$. The two layers consist of silicon microstrips detectors oriented in orthogonal directions with a readout pitch of $242 \mu\text{m}$, but with the floating strip design. All planes (except the last two planes) contain a Tungsten layer of $245 \mu\text{m}$ ($0.07 X_0$). We modeled also the mechanical supports, the Aluminum honeycomb structure, the front-end electronics chips and other tray components. In our simulations, we make a crucial use of a parametrization of the capacitive coupling among contiguous Si-microstrips. Our parametrization reproduce the experimental data obtained at a CERN test beam in May 2000 [4, 5]. The Mini-Calorimeter is modeled by two planes, each containing 16 CsI bars oriented orthogonally. The bars are 1.4 cm thick and have a width of 2.4 cm. The Anticoincidence (AC) system is made of a top panel of plastic scintillator ($\sim 54 \times 54 \times 0.5 \text{ cm}^3$) and 3 panels for each lateral side of the AGILE Tracker ($\sim 18.1 \times 44.4 \times 0.6 \text{ cm}^3$). We also included a simplified description of the photomultipliers, GRID readout electronics, and mechanical structure.

Super-AGILE. The Super-AGILE detector layer is made of 16 Silicon detectors that are similar to those used for the Tracker. A gold mask ($\sim 90 \mu\text{m}$ thick) is placed at a distance of 14 cm from the active detector plane, and is supported by a light structure of Au-coated Carbon fibers acting as collimator for 10–40 keV X-rays. We studied in detail the background induced on the GRID by Super-AGILE.

Fig. 1 shows a simplified view of the AGILE instrument model used in our simulations.

BACKGROUND ASSUMPTIONS

Charged particle background

A quasi-equatorial orbit is preferred for the AGILE mission and will provide a relatively low-background environment. Taking into account data from SAS-2 and Beppo-SAX missions, we expect an average rate of charged particle background above ~ 1 MeV of ~ 0.3 particles $\text{cm}^{-2} \text{s}^{-1}$ for a quasi-equatorial orbit near 550 km. The charged particle background for this orbit is known to be relatively stable, with an increase by a factor 10-100 near the South Atlantic Anomaly. The charged particle energy spectra assumed in our simulations are shown in Fig. 2. They are based on data from the 1998 AMS Shuttle flight [6, 7], and from the MARYA experiment on board of the MIR space station [8]. These data were selected for events detected near the geomagnetic equator, and their low-energy extrapolations are consistent with the total rates detected by SAS-2 and Beppo-SAX. We used the correct angle distributions for different particle components: an isotropic distribution for electrons, positrons and trapped protons, and an upper-hemispheric distribution for primary protons (for a zenithal AGILE pointing).

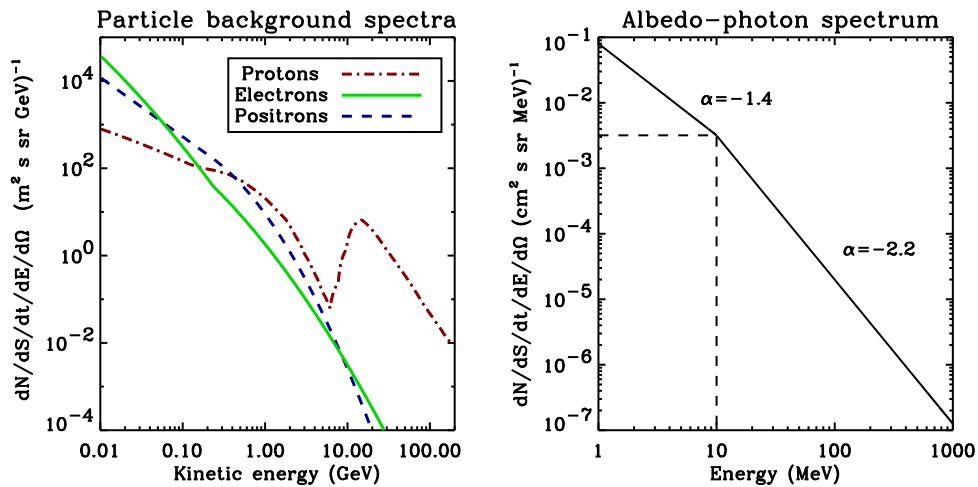


FIGURE 2. *Left Panel:* Charged particle background energetic spectra (from [6, 7, 8]) assumed in our simulations. *Right Panel:* Average albedo-photon energy spectrum (from [9, 10]).

Albedo-photon background

The interaction of the charged cosmic-rays with the upper atmosphere induces a relatively strong gamma-ray background peaking at the Earth horizon. This effect involves a localized increase of the gamma-ray emission that we properly took into account on the basis of SAS-2 [9] and other balloon data [10]. Fig. 2 shows the average flux of albedo photons over the solid angle of the subtended Earth surface at the height of 550 km.

TRIGGER STRATEGIES AND BACKGROUND REJECTION

We studied different GRID trigger configurations, and optimized their performance. The baseline GRID trigger logic consists of two different levels. A (hardware) Level-1 trigger logic uses the information from the Silicon detectors and AC panels and considers also a simplified view of the event topology obtained by the front-end chips. Level-1 trigger reduces the charged-particle background from a rate of ~ 2000 Hz to a rate of ~ 60 Hz. A (software) Level-2 on-board data processing makes a crucial use of the analog (charge) information in the Si-microstrips for a refined view of the event topology at the “cluster” level. Level-2 on-board processing also selects events based on a simplified photon direction reconstruction (necessary to reject Earth albedo photons). After the on-board Level-2 processing, we can reduce the total (charged particle and albedo-photon) background rate to $\sim 20 - 30$ Hz.

EFFECTIVE AREA

Using the trigger logic outlined in the previous section, we studied the AGILE-GRID efficiency to detect gamma-rays at different incidence angles and energies. The effective area is, by definition: $A_{eff} = \epsilon A_{\perp}$, where A_{\perp} is the detector “geometrical area” (equivalent area perpendicular to the incident flux direction) and ϵ is the detector efficiency, given by the product $\epsilon = \epsilon_i \cdot \epsilon_t \cdot \epsilon_r$, with ϵ_i the photon interaction probability, ϵ_t the trigger efficiency, and ϵ_r the photon event reconstruction efficiency.

The GRID effective area after Level-2 processing (without the photon-event reconstruction cut) is shown in Fig. 3. The GRID is characterized by an excellent performance off-axis, and by an effective area smaller by a factor of 2 than that of EGRET for on-axis events.

CONCLUSIONS

Our simulations show that the mechanical and electronic design of the GRID is appropriate for an efficient background rejection and optimized scientific performance. Despite its small volume and mass, the AGILE-GRID will reach a very good sensitivity and wide angle event acceptance. For each pointing, the GRID field of view will be unprecedentedly large, $\sim 1/5$ of the entire sky, for observations above 30 MeV.

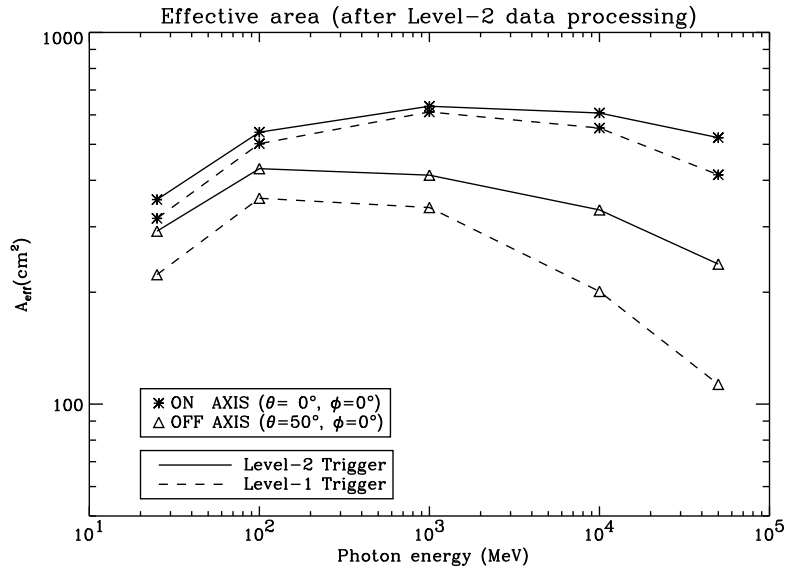


FIGURE 3. AGILE effective area after on-board Level-2 data processing (without photon event reconstruction efficiency to be obtained after an off-line data analysis. Simulations results from ref. [11, 12]).

We acknowledge the joint work and contributions to the material presented in this paper by G. Fedel, P. Lipari, and A. Pellizzoni.

REFERENCES

1. Tavani M. et al., these Proceedings
2. Giani S. et al., CERN Long Writup W5013 (1994)
3. Barbiellini G. et al., these Proceedings
4. Fedel G. et al., *X-Ray and Gamma-Ray Instrumentation for Astronomy XI*, Flanagan K.A. and Siegmund O.H.W. eds., SPIE Conference Proceedings 4140, 274, (2000)
5. Barbiellini G. et al., NIM-A submitted, INFN/TC-01/006 (2001)
6. Alcaraz J. et al., Physics Letters B 472, 215 (2000)
7. Alcaraz J. et al., Physics Letters B 484, 10 (2000)
8. Koldashov S.W. et al., 24th ICRC 4, 993, (1995)
9. Thompson D.J., Simpson G.A. and Özel M.E., Journal of Geophysical Research 86, 1265 (1981)
10. Costa E., Massaro E., Salvati M. and Appolloni A., Astrophysics and Space Science 100, 165 (1984)
11. Longo F., Cocco V. and Tavani M. (2001), in preparation
12. Cocco V., Longo F. and Tavani M. (2001), in preparation